Isotropic-nematic interface of liquid-crystalline polymers

Shi-Min Cui*
Department of Physics, University of Waterloo, Waterloo, Ontario, Canada N2L 3G1

Osman Akcakir and Zheng Yu Chen
Guelph-Waterloo Program for Graduate Work in Physics and Department of Physics, University of Waterloo Waterloo, Ontario, Canada N2L 3G1

(Received 28 November 1994)

The behavior of liquid crystalline polymers in the interfacial region between the isotropic and nematic phases is investigated based on an inhomogeneous free-energy functional. A mean-field approximation is used for the system of semiflexible polymers obeying the Saito-Takahashi-Yunoki description and interacting via the Onsager-type repulsive interaction. The density distribution of the polymers crossing the interface is computed by using a spherical-harmonics expansion. The calculated interfacial tension is consistent with the results of the scaling argument which is also presented in this paper.

PACS number(s): 64.70.Md, 68.10.Cr, 61.30.Cz

I. INTRODUCTION

The development of orientational order near the interface in liquid-crystalline materials has been the focus of theoretical and experimental investigation during the past decades for fundamental reasons and technical importance [1–15]. Due to the coupling between the angular order parameter and the molecular concentration, many interesting features can occur; the coupling, however, also introduces difficulties in establishing and solving models for this type of system [2,5–13].

Our main concern here is the interface between the isotropic (I) and nematic (N) states of a lyotropic system. Several theoretical studies have been reported for the isotropic-nematic interface of the rigid-rod systems [6–13]. In these studies, the spatial variation of the interface profile is induced by considering the Onsager-type rod-rod interaction at different positions in space. It is found that the interfacial width is of order L, the length of the rods. The rigid-rod model is of limited utility for liquid-crystalline polymers, since most liquid-crystalline polymers are semiflexible, not rigid.

The importance of studying the isotropic-nematic interface of semiflexible liquid-crystalline polymers was first stressed by Grosberg and Pachomov [11]. The main length scale in the Onsager-type interaction for different orientational regions is now approximately the Kuhn length a. The interfacial width is expected to have the same order, regardless of the total contour length of the polymer chain L. The strength of the interaction is of order D, where D is the diameter for the excluded volume interaction. The interfacial problem of liquid-crystalline polymers is quite different from that of, say, immiscible polymer A and polymer B [16]. For the latter, the size of the interface is approximately of the order of the radius of gyration $(aL)^{1/2}$. Although the liquid-crystalline interface is much narrower, it is still much wider than the interface of low-molecular-weight systems; for persistent chains, the Kuhn length can be as large as a few hundred times the basic monomer length scale.

Presently, several general theories that contain ambiguous or nonrealistic parameters are available for semiflexible polymers [17–19]. However, none of them deals with a concrete model that can give results comparable to experiments. To understand the problem at the molecular level, we have established a mean-field model based on the Saito-Takahashi-Yunoki description [20] for semiflexible polymers. For the bulk properties at the flexible limit [21], the model recovers that of Khokhlov and Semenov (KS) [22], who extended the Onsager theory [23] to very long semiflexible chains in order to describe the isotropic-nematic transition.

In the present paper, we study the isotropic-nematic interface of flexible polymers assuming that the chains interact with each other only via hard-core repulsion. Our basic technique to solve the model is to maintain coefficients of the high-order terms in the expansion of the distribution function in terms of the spherical harmonics; these coefficients are spatially varying. We rely on numerical computation to exactly calculate the interfacial profile, thus avoiding the pitfalls of other approximation methods [5–11,17,18,24].

This paper is organized as follows. In Sec. II, we present a qualitative discussion and scaling argument of the problem. In Sec. III, we specify the model and provide the basic analytic formulas. In Sec. IV, we present the numerical results and discussions.

II. SCALING ARGUMENT

In this section, we discuss a qualitative consideration that yields the scaling properties for various physical quantities. A more rigorous formulation of an exact

*Permanent address: Department of Applied Physics, Jiao Tong University, Shanghai 200030, People's Republic of China.

theory will be presented in the next section.

We are mainly interested in flexible chains with a homogeneous distribution of flexibility along the chain, i.e., the wormlike model in the flexible limit. Qualitatively, the physical behavior of the system should be similar to that of a system consisting of the same number of molecules described by the freely jointed model. In such a model, a polymer chain is regarded as being made up of L/a rigid rods, while the junction between the two consecutive rods is assumed to be freely jointed. Since there is no entropy cost associated with these junctions, the orientational entropy of the system consisting of N molecules, each having L/a rod segments, is the same as the system consisting of NL/a freely moving, disconnected rods of length a. For the latter, let us assume that we can use the Onsager model that concludes that when the number density of rods reaches the transition number density of order $C_{\text{rods}} \approx 5/a^2 D$, a first-order isotropic-nematic transition takes place [25]. Using this analogy, we can estimate that the I-N transition for the system of freely rotating rods will take place near the molecular number density $C_{\text{chains}} = C_{\text{segments}}/(L/a) = (5/a^2 D)/(L/a)$. Indeed, the exact result for wormlike chains at the $L/a \gg 1$ limit shows a transition density of the same order with a somewhat larger coefficient [21,26]. The difference in the coefficients is caused by taking into consideration the orientational entropy between the two persistent segments.

Now we turn our attention to a qualitative discussion for the I-N interface. As mentioned earlier, the width of the interface should be of order a. Assume that one segment of the chain is dispatched across the interface region from the I phase to the N phase. The free-energy change due to the entropy increase is of order $k_B T$. There are, in total, aAC_{segments} segments for an interface area A. The interfacial tension is then approximately $k_B T a A C_{\text{segments}}/A \propto k_B T/aD$. Note that the interfacial tension is inversely proportional to the Kuhn length a and is *independent* of the total chain length L. Our calculation below supports this scaling behavior.

The change in density profile across the interface is penalized by a translational entropy term in the free energy. A prototypical example of such a term is the Cahn-Hilliard-like square-gradient term [27] described by the operator $(\mathbf{u}\cdot\nabla_{\mathbf{r}})^2$ [6,9], where $\mathbf{u}$ is the orientational variable for the polymer segments. In an idealized picture for qualitative analysis, the orientational distribution of the N phase could be imagined to be of a δ-function form. In such an approximation, all segments are perfectly aligned. The above square-gradient operator can then be represented by the term $\cos^2(\mathbf{u}\cdot\mathbf{n})$ where $\mathbf{n}$ is the normal of the interface. In order to minimize the surface tension, a square-gradient term will naturally lead to a preferred tilt angle $\mathbf{u}\cdot\mathbf{n} = \pi/2$, a result consistent with the quantitative analysis to be described in Sec. IV. It was questioned by Moore and McMullen [10] whether or not a square-gradient expansion is sufficient for describing the orientational interfacial problem such as the one considered here. Our model is based on a closed-form approach that contains, in principle, all expanded terms. From our exact result, it can be seen that the high-order gradient correction terms to the square-gradient term would not affect the conclusion drawn here regarding the preferred tilt angle.

III. BASIC FORMALISM

In this section, we develop the basic formalism for the problem. Consider a spatially inhomogeneous system of semiflexible polymer chains. The distribution function of polymer segments with contour variable t depends on both the spatial and orientational variables. Let $\rho(\mathbf{r},\mathbf{u})$ be the contour-averaged number density of the chains at the point $\mathbf{r}$, having the orientation specified by the unit vector $\mathbf{u}$. In a self-consistent mean-field theory, the grand thermodynamical potential function Ω of the system can be expressed in terms of the distribution $\rho(\mathbf{r},\mathbf{u})$ and the mean field $w(\mathbf{r},\mathbf{u})$ representing the averaged effects of the neighboring chains

$$\frac{\Omega}{k_B T} = -\int d\mathbf{r}\, d\mathbf{u}\, w(\mathbf{r},\mathbf{u})\rho(\mathbf{r},\mathbf{u}) + \frac{L^2 D}{2}\int d\mathbf{r}\, d\mathbf{u}\, d\mathbf{u}'\rho(\mathbf{r},\mathbf{u})\rho(\mathbf{r},\mathbf{u}')|\mathbf{u}\times\mathbf{u}'| - \mu\int d\mathbf{r}\, d\mathbf{u}\,\rho(\mathbf{r},\mathbf{u}) , \tag{1}$$

where μ is the chemical potential, L and D are the total contour length and the diameter of a polymer chain. In Eq. (1), the first term stands for the conformational entropy and the second term represents the excluded-volume interaction between segments of the polymer chains, where we have assumed the second virial approximation. Minimization of Eq. (1) with respect to $\rho(\mathbf{r},\mathbf{u})$ yields the interfacial profile $\rho(\mathbf{r},\mathbf{u})$.

The relationship between the mean field and the density distribution is governed by a second-order partial differential equation, described in detail in the Appendix. There it is shown that the mean field for the limit $L/a \gg 1$ can be expressed as

$$w(\mathbf{r},\mathbf{u}) = \frac{L}{a}\frac{\nabla_u^2 q(\mathbf{r},\mathbf{u})}{q(\mathbf{r},\mathbf{u})} - L\frac{\mathbf{u}\cdot\nabla_{\mathbf{r}} q(\mathbf{r},\mathbf{u})}{q(\mathbf{r},\mathbf{u})} , \tag{2}$$

where $q(\mathbf{r},\mathbf{u})$ is an auxiliary function related to $\rho(\mathbf{r},\mathbf{u})$ by

$$\rho(\mathbf{r},\mathbf{u}) = q(\mathbf{r},-\mathbf{u})q(\mathbf{r},\mathbf{u}) . \tag{3}$$

The spatial variation is indirectly introduced through the last term in Eq. (2). It is not obvious that the free-energy model in Eqs. (1)–(3) can be expanded in a *square-gradient* series because of the appearance of the first-order operator $\nabla_{\mathbf{r}}$. One can show that by introducing a spherical-harmonics expansion for the angular dependence and a weak $\nabla_{\mathbf{r}}$ expansion for the spatial dependence, Eq. (1) can be rewritten in a more conventional square-gradient form.

Before we proceed further in solving the proposed problem, we would like to point out a symmetry property of the model. From Eq. (3), an inversion symmetry for the distribution function always exists,

$$\rho(\mathbf{r},\mathbf{u}) = \rho(\mathbf{r},-\mathbf{u}) . \tag{4}$$

Since a thermodynamic potential function should be in-

variant under symmetry transformations [28], Eq. (1) implies that the same inversion symmetry also exists for the mean field,

$$w(\mathbf{r},\mathbf{u})=w(\mathbf{r},-\mathbf{u}) . \tag{5}$$

One should note, however, that the function $q(\mathbf{r},\mathbf{u})$ lacks the inversion symmetry in general. Other special symmetry properties that can be deduced for special cases will be discussed below.

A. Bulk phases

The bulk properties for the phase transition have been studied and reported by several authors [21,22,26,29]. Here for completeness, we review the main results.

For the case of a spatially homogeneous phase, $\rho(\mathbf{r},\mathbf{u})$ and $q(\mathbf{r},\mathbf{u})$ become independent of the position: $\rho(\mathbf{r},\mathbf{u})=\rho_b(\mathbf{u})$, $q(\mathbf{r},\mathbf{u})=q_b(\mathbf{u})$. The inversion symmetry of the mean-field function in Eqs. (2)–(5) implies

$$q_b(\mathbf{u})=q_b(-\mathbf{u}) , \tag{6}$$

which is only valid for the spatially uniform case. Furthermore, the nematic state is assumed to be uniaxial, so that one can conveniently define the polar variable θ measured from the nematic director [1].

The free-energy model in Eqs. (1)–(3) reduces to the KS model for the isotropic-nematic phase transition [22],

$$\frac{a\Omega}{k_BTLV}=-\int d\mathbf{u}\, q_b(\mathbf{u})\nabla_{\mathbf{u}}^2 q_b(\mathbf{u}) + \frac{aLD}{2}\int d\mathbf{u}\, d\mathbf{u}'\rho_b(\mathbf{u})\rho_b(\mathbf{u}')|\mathbf{u}\times\mathbf{u}'| - \bar{\mu}\int d\mathbf{u}\,\rho_b(\mathbf{u}) , \tag{7}$$

where $\bar{\mu}=a\mu/L$ and V is the system volume.

There are at least three procedures that have been used to minimize the grand potential in Eq. (7). The first, as was used by several authors, is the variational method. The function $\rho(\mathbf{u})$ in Eq. (7) is substituted by an artificially imposed form similar to that proposed by Onsager [23] for rigid rods

$$\rho_b(\mathbf{u})\sim\cosh(\beta\cos\theta) ,$$

where θ is the polar variable; the minimization procedure is then approximated by minimizing the free energy with respect to the variational parameter β [22,29].

The second method is based on a direct minimization of Eq. (7) with respect to the unknown distribution function $\rho_b(\mathbf{u})$. The variable space for the spherical polar variable θ is discretized and the distribution function is represented by a series of numbers at these discretized points. An efficient numerical algorithm can be established based on this method [21]. However, it is difficult to generalize this method to study the interfacial properties due to the difficulty in handling a large number of variables; that would lead to extensive computations.

The third method is also based on a direct minimization of Eq. (7), but with respect to the unknown distribution function $q_b(\mathbf{u})$, which is expanded in terms of the spherical harmonics [26]. It is this method that we have adopted to analyze the interfacial problem, thus we give here a detailed derivation.

The minimization condition for the grand thermodynamical potential is a nonlinear integrodifferential equation:

$$[-\nabla_{\mathbf{u}}^2+aLD\int d\mathbf{u}' q_b(\mathbf{u}')q_b(\mathbf{u}')|\mathbf{u}\times\mathbf{u}'|-\bar{\mu}]q_b(\mathbf{u})=0 . \tag{8}$$

Due to the rotational symmetry of the system around the nematic director, this integrodifferential equation can be attacked by expanding all terms in Legendre polynomials. The inversion symmetry of $q_b(\mathbf{u})$ in Eq. (6) implies that all coefficients of the odd-order Legendre functions are zero. For later convenience we write the expansion in terms of the spherical harmonics [30],

$$q_b(\mathbf{u})=\frac{1}{\sqrt{aLD}}\sum_{l=0}^{\infty} q_{b,2l}Y_{2l,0}(\mathbf{u}) , \tag{9}$$

where $q_{b,2l}$ is dimensionless. To expand the excluded-volume interaction term, we make use of the spherical-harmonic expansion of the kernel $|\mathbf{u}\times\mathbf{u}'|$, which can be obtained by using the addition theorem [30]

$$|\mathbf{u}\times\mathbf{u}'|=\sum_{l=0}^{\infty}\sum_{m}\frac{4\pi}{4l+1}d_{2l}Y_{2l,m}(\mathbf{u})Y_{2l,m}^{*}(\mathbf{u}') , \tag{10}$$

where

$$d_0=\frac{\pi}{4} , \tag{11a}$$

$$d_{2l}=-\frac{\pi(4l+1)(2l)!(2l-2)!}{2^{4l+1}(l-1)!l!l!(l+1)!} , \quad (l\geq 1) . \tag{11b}$$

Now from Eq. (8) one has

$$[2l(2l+1)-\bar{\mu}]q_{b,2l}+\sum_{l_2,l_3,l_4}\left[\sum_{l_1}\frac{8\pi}{4l_1+1}d_{2l_1}I_{2l,2l_1,2l_2}I_{2l_1,2l_3,2l_4}\right]q_{b,2l_2}q_{b,2l_3}q_{b,2l_4}=0 , \tag{12}$$

where

$$I_{2l_1,2l_2,2l_3}=\left[\frac{(4l_1+1)(4l_2+1)}{4\pi(4l_3+1)}\right]^{1/2}\times[C(2l_1,2l_2,2l_3;0,0,0)]^2 , \tag{13}$$

and $C(l_1,l_2,l_3;m_1,m_2,m_3)$ is the Clebsch-Gordan coefficient. The chemical potential used in the coexistence condition of the isotropic and nematic phases can be expressed as

$$\bar{\mu}=2\pi\left[\sum_{l=0}\frac{d_{2l}}{4l+1}\left[\sum_{l_1,l_2}I_{2l,2l_1,2l_2}q_{b,2l_1}q_{b,2l_2}\right]^2\right]^{1/2} . \tag{14}$$

The hierarchy of the coupled, nonlinear algebraic equations in Eq. (12) must be truncated at a certain order for actual computation. Vroege and Odijk [26] used the fixed-point iteration technique to solve Eq. (12) for a given $\bar{\mu}$. The equations must be manipulated in order to make the computation procedure convergent. Here we use a different technique; the Newton algorithm for solving a set of nonlinear equations is applied.

The expansion truncated at $2l=10$ gives rise to the value of the chemical potential at the phase equilibrium

$$\bar{\mu}=20.4935 \ . \tag{15}$$

The expansion truncated at $2l=20$ gives rise to $\bar{\mu}=20.4926$ [26]. Therefore, we consider it sufficient to truncate all the series expansions at $2l=10$ in our computation. We try to maintain a small number of spherical-harmonic coefficients, because the interfacial problem involves a large number of variables for additional spatial dependence. The harmonic coefficients $q^N_{b,2l}$ in Eq. (9) for the homogeneous nematic phase are summarized in Table I. For the isotropic phase only the $l=0$ coefficient is nonzero. For comparison, we have also listed the result obtained by Vroege and Odijk [26] when the series is truncated at a much higher order. While these authors found that the fixed-point iteration algorithm gives two possible solutions for the nematic state when $\bar{\mu}<17.50$, we found only one solution by using the Newton algorithm.

Truncating at $2l=10$ leads to the coexistence concentration boundary given by

$$C_I=aLD\int d\mathbf{u}\rho^I_b(\mathbf{u})=13.047 \tag{16}$$

and

$$C_N=aLD\int d\mathbf{u}\rho^N_b(\mathbf{u})=14.028 \ , \tag{17}$$

and the orientational order parameter S^N of the nematic phase given by

$$S^N=\langle P_2(\cos\theta)\rangle=0.4615 \ . \tag{18}$$

TABLE I. The expansion coefficients for the bulk phases.

Coefficient	Vroege and Odijk [26]	This work
q^I_0	3.611 954	3.612 004
q^N_0	3.289 032	3.289 341
q^N_2	1.774 425	1.773 986
q^N_4	0.247 511	0.247 362
q^N_6	$2.058\,18\times10^{-2}$	$1.975\,55\times10^{-2}$
q^N_8	1.2152×10^{-3}	1.2136×10^{-3}
q^N_{10}	6.6548×10^{-5}	6.6344×10^{-5}
q^N_{12}	3.4577×10^{-6}	0
q^N_{14}	1.7411×10^{-7}	0
q^N_{16}	8.556×10^{-9}	0
q^N_{18}	4.118×10^{-10}	0
q^N_{20}	1.95×10^{-11}	0

These results are in agreement with more accurate results: $C_I=13.046$, $C_N=14.029$, and $S^N=0.4618$ [21,26].

B. Isotropic-nematic interface

The inhomogeneous interface represents a much more complicated computational problem. The rotational symmetry and the inversion symmetry of the q function are destroyed. The free-energy model in Eqs. (1)–(3) must be solved by taking the spatial variable $\mathbf{r}$, the polar angle θ, and the azimuthal angle ϕ into consideration.

We have chosen the coordinate system as in Fig. 1. For the spatial variable, the x axis is along the normal to the flat isotropic-nematic interface; the system is translationally invariant in the y and z directions. Thus, the distribution function only depends on x spatially. The polar variables to describe $\mathbf{u}$ are defined in the tilted coordinate frame labeled by the Cartesian variables u_x, u_y, and u_z. The direction of the u_z coordinate coincides with the bulk nematic director, so that the angle between the direction of the u_z axis and the normal to the interface is the tilt angle θ_t. The u_y direction is chosen in the same direction as the y axis. We can then rewrite the grand-potential functional (1) in the form

$$\frac{\Omega}{k_BTLA}=-\int dx\,d\mathbf{u}\,q(x,-\mathbf{u})\nabla^2_{\mathbf{u}}q(x,\mathbf{u})+\int dx\,d\mathbf{u}\,q(x,-\mathbf{u})(\cos\theta_t u_z+\sin\theta_t u_x)\frac{\partial q(x,\mathbf{u})}{\partial x}$$
$$+\frac{aLD}{2}\int dx\,d\mathbf{u}\,d\mathbf{u}'\rho(x,\mathbf{u})\rho(x,\mathbf{u}')|\mathbf{u}\times\mathbf{u}'|-\bar{\mu}\int dx\,d\mathbf{u}\,\rho(x,\mathbf{u}) \ , \tag{19}$$

where A is the area of the interface. Note that in Eq. (19) we have used the rescaled variable x which is in the units of the Kuhn length a.

In the following analysis, the tilt angle θ_t in the second term is fixed to several given values in order to examine the effect of a nontrivial tilt angle. The minimization procedure leads to an integrodifferential equation

$$[-\nabla^2_{\mathbf{u}}+(\cos\theta_t u_z+\sin\theta_t u_x)\frac{\partial}{\partial x}$$
$$+aLD\int d\mathbf{u}'\rho(x,\mathbf{u}')|\mathbf{u}\times\mathbf{u}'|-\bar{\mu}]q(x,\mathbf{u})=0 \ , \tag{20}$$

that needs to be solved for the flat interface. The boundary conditions are imposed so that at the $x\to+\infty$ limit one has the nematic phase and at the $x\to-\infty$ limit the isotropic phase

$$q(x,\mathbf{u})=\begin{cases} q^I_b \ , & x\to-\infty \ , \\ q^N_b(\mathbf{u}) \ , & x\to+\infty \ . \end{cases} \tag{21}$$

For an arbitrary θ_t it can be seen from Eq. (19) that $q(x,\mathbf{u})$ has the following symmetry properties:

$$q(x,\mathbf{u})=q^*(x,\mathbf{u})=q(x,\mathbf{u}_{\sigma_y}) \ , \tag{22}$$

where $\mathbf{u}_{\sigma_y}=(\theta,-\phi)$ is the mirror image of $\mathbf{u}=(\theta,\phi)$ when the $u_y=0$ plane is considered to be the reflection mirror.

The partition function $q(x,\mathbf{u})$ can be expressed in terms of the spherical harmonics $Y_{l,m}(\mathbf{u})$,

$$q(x,\mathbf{u})=\frac{1}{\sqrt{aLD}}\sum_{l=0}\sum_{m}q_{l,m}(x)Y_{l,m}(\mathbf{u})\ . \tag{23}$$

We find from the symmetry properties in Eq. (20) that the coefficients $q_{l,m}$ obey

$$q_{l,m}(x)=q^{*}_{l,m}(x)=(-1)^{m}q_{l,-m}(x)\ . \tag{24}$$

By using these symmetry properties, we can reduce the number of independent variables in the actual calculation. Note that the coefficients of the spherical harmonics of odd l index in Eq. (23) are now nonzero.

We now multiply both sides of Eq. (20) by $Y^{*}_{l,m}(\mathbf{u})$ and integrate over $\mathbf{u}$. This procedure yields

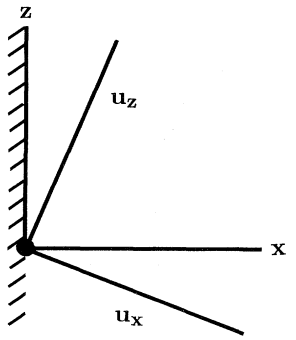

FIG. 1. Definition of the coordinate system. The spherical polar coordinates for describing $\mathbf{u}$ are defined in the $\mathbf{u}$-coordinate frame. The interface normal is along the x direction and the bulk nematic director is along the u_z direction. The y direction coincides with the u_y direction, which is specified by the filled circle at the origin.

$$\begin{aligned}[l(l+1)-\bar{\mu}]q_{l,m}(x)-\sin(\theta_t)&\left[J_{l+1,m+1}\frac{\partial q_{l+1,m+1}(x)}{\partial x}+J_{l,m}\frac{\partial q_{l-1,m-1}(x)}{\partial x}-J_{l+1,1-m}\frac{\partial q_{l+1,m-1}(x)}{\partial x}\right.\\&\left.-J_{l,-m}\frac{\partial q_{l-1,m+1}(x)}{\partial x}\right]\\+\cos(\theta_t)&\left[J'_{l+1,m}\frac{\partial q_{l+1,m}(x)}{\partial x}+J'_{l,m}\frac{\partial q_{l-1,m}(x)}{\partial x}\right]\\+\sum_{\mathbf{l},\mathbf{m}}&\frac{8\pi}{4l_1+1}(-1)^{l_4+m}d_{2l_1}q_{l_2,m_2}(x)q_{l_3,m_3}(x)q_{l_4,m_4}(x)I_{l,-m,2l_1,m_1,l_2,m_2}I_{2l_1,-m_1,l_3,m_3,l_4,m_4}=0\ ,\end{aligned} \tag{25}$$

where the boldfaced indices $\mathbf{l}$ and $\mathbf{m}$ indicate that the sum is over all relevant values of l_1, l_2, l_3, l_4, m_1, m_2, m_3, and m_4. The constants J, J', and I are known,

$$J_{l,m}=\frac{1}{2}\left[\frac{(l+m)(l+m-1)}{(2l+1)(2l-1)}\right]^{1/2}, \tag{26a}$$

$$J'_{l,m}=\left[\frac{(l+m)(l-m)}{(2l+1)(2l-1)}\right]^{1/2}, \tag{26b}$$

and

$$\begin{aligned}I_{l_1,m_1,l_2,m_2,l_3,m_3}=(-1)^{m_3}&\left[\frac{(2l_1+1)(2l_2+1)}{4\pi(2l_3+1)}\right]^{1/2}\\&\times C(l_1,l_2,l_3;0,0,0)\\&\times C(l_1,l_2,l_3;m_1,m_2,-m_3)\ .\end{aligned} \tag{26c}$$

The harmonic coefficients $q_{l,m}(x)$ must obey the boundary conditions

$$q_{l,m}(x)=\begin{cases}q^{I}_{b,l,m}\ , & x\to-\infty\ ,\\ q^{N}_{b,l,m}\ , & x\to+\infty\ ,\end{cases} \tag{27}$$

where $q^{I(N)}_{b,l,m}$ are those listed in Table I. The nonlinear integrodifferential equation (20) is now represented by an infinite number of nonlinear algebraic equations that contain unknown variables $q_{l,m}$.

In practice, we truncate the expansion in Eq. (23) after the $l=10$ term. Because of Eq. (24), there are only $n_l=(l+1)(l+2)/2=66$ independent functions $q_{l,m}(x)$ that need to be considered. We assume that these functions approach their asymptotic bulk-phase values exponentially fast, so that we redefine a spatial variable ξ by

$$\xi=\tanh(x/2)\ . \tag{28}$$

The differential term in Eq. (25) can be rewritten as $\partial q_{l,m}/\partial x=\frac{1}{2}(1-\xi^2)\partial q_{l,m}/\partial\xi$. The interval $x=[-\infty,\infty]$ now becomes $\xi=[-1,1]$. In order to represent the spatial variation, we use $n_\xi=50$ equally spaced discrete points in the interval $[-1,1]$ for ξ with a mesh width $\Delta\xi=0.04$. The derivative of $q_{l,m}(\xi)$ with respect to ξ is approximated by using a finite difference scheme. The corresponding discretization for the variable x is nonuniform; more points are considered near the interface and fewer points farther away. A step function centered at $x=0$ is assumed for the initial guess of the interfacial profile and the values $q_{l,m}$ obtained for bulk phases are chosen to be the initial approximation for each side of the step functions. The chemical potential is chosen to be that for the coexistence condition, $\bar{\mu}=20.493$. At each step of the numerical iteration, the $n_l(n_\xi+1)=3366$ nonlinear equations are linearized by using the guessed profile as the reference one. The linear

equations are solved for the $n_l(n_\xi+1)=3366$ variables and the result is used as the new guess for the next step of iterations. This procedure involves the inversion of a large matrix of order 3366. The matrix can be expressed in a block tridiagonal form so that the block-elimination method can be used [31]. The iteration is assumed to converge when the right-hand side of Eq. (25) deviates from zero with a relative precision of 5×10^{-4}. This method has proved to be quite efficient, and it converges to the given accuracy in less than ten iteration steps.

IV. RESULTS

We can use the functions $q_{l,m}(x)$ to compute the number density profile, the order-parameter profile, the biaxiality profile, the interface tension, etc. For this purpose, we need to consider the density distribution

$$\rho(x,\mathbf{u})=\frac{1}{aLD}\sum_{l=0}\sum_{m}\rho_{l,m}(x)Y_{l,m}(\mathbf{u}) , \tag{29}$$

in which the coefficients $\rho_{l,m}(x)$ can already be deduced from $q_{l,m}(x)$

$$\rho_{l,m}(x)=\sum_{l_1,l_2}\sum_{m_1,m_2} I_{l,-m,l_1,m_1,l_2,m_2}(-1)^{l_1+m} \times q_{l_1,m_1}(x)q_{l_2,m_2}(x) . \tag{30}$$

Integrating $\rho(x,\mathbf{u})$ over the spherical polar variables, we find the spatial variation for the number density

$$c(x)=aLD\int d\mathbf{u}\,\rho(x,\mathbf{u})=(4\pi)^{1/2}\rho_{0,0} . \tag{31}$$

The degree of orientational order is characterized by the statistical average of the tensor $\frac{1}{2}(3\mathbf{uu}-\mathbf{I})$ [1],

$$\mathcal{S}(x)=\frac{1}{2}\int d\mathbf{u}(3\mathbf{uu}-\mathbf{I})\rho(x,\mathbf{u})/\int d\mathbf{u}\,\rho(x,\mathbf{u}) =\frac{1}{2\sqrt{5}\rho_{0,0}}\begin{bmatrix}\sqrt{6}\rho_{2,2}-\rho_{2,0} & 0 & \sqrt{6}\rho_{2,1}\\ 0 & -(\sqrt{6}\rho_{2,2}+\rho_{2,0}) & 0\\ \sqrt{6}\rho_{2,1} & 0 & 2\rho_{2,0}\end{bmatrix} . \tag{32}$$

In the interfacial region the tensor order parameter in Eq. (32) contains nonzero functions $\rho_{2,2}(x)$ and $\rho_{2,1}(x)$, which symbolize the appearance of the biaxiality and the variation of the principle nematic axis, respectively. Diagonalizing the matrix in Eq. (32)

$$\mathcal{U}\mathcal{S}\mathcal{U}^{-1}=\begin{bmatrix}\frac{1}{2}(P-S) & 0 & 0\\ 0 & -\frac{1}{2}(P+S) & 0\\ 0 & 0 & S\end{bmatrix} , \tag{33}$$

enables us to identify the principle order parameter $S(x)$ and the biaxiality parameter $P(x)$

$$S(x)=\frac{1}{4\sqrt{5}\rho_{0,0}}[\rho_{2,0}+\sqrt{6}\rho_{2,2}+(9\rho_{2,0}^2+6\rho_{2,2}^2+24\rho_{2,1}^2 -6\sqrt{6}\rho_{2,0}\rho_{2,2})^{1/2}] , \tag{34}$$

and

$$P(x)=\frac{1}{4\sqrt{5}\rho_{0,0}}[3\rho_{2,0}+\sqrt{54}\rho_{2,2}-(9\rho_{2,0}^2+6\rho_{2,2}^2+24\rho_{2,1}^2 -6\sqrt{6}\rho_{2,0}\rho_{2,2})^{1/2}] . \tag{35}$$

The deviation angle $\gamma(x)$ between the local nematic director at x and the bulk nematic director at $x=\infty$ can also be calculated using the diagonalization matrix $\mathcal{U}$

$$\tan\gamma(x)=[(1.5\rho_{2,0}^2+\rho_{2,2}^2+4\rho_{2,1}^2-\sqrt{6}\rho_{2,0}\rho_{2,2})^{1/2} -\sqrt{1.5}\rho_{2,0}+\rho_{2,2}]/2\rho_{2,1} . \tag{36}$$

The interfacial tension σ can be calculated by considering the difference between the grand thermodynamic potential of the interface in Eq. (19) and that of the homogeneous, isotropic phase. Written in terms of ρ, σ is expressed as

$$\frac{\sigma}{k_BT}=\frac{2\pi}{aD}\int_{-\infty}^{+\infty}dx[d_0(\rho_{0,0}^I)^2 -\sum_{l=0}\sum_{m}\frac{(-1)^m}{4l+1}d_{2l}\rho_{2l,m}^2] , \tag{37}$$

The actual integration is carried out by substituting the variable ξ in Eq. (37) and implementing the Simpson rule for integration over ξ.

The profiles of the density $c(x)$, the order parameter $S(x)$, the biaxiality $P(x)$, and the deviation angle $\gamma(x)$ are calculated for different values of the tilt angle and are plotted as functions of x in Fig. 2. The centers of each of the density profiles in Fig. 2(a) are consecutively shifted by a from the previous one for each given θ_t in order to display all five figures in one plot. The relative positions between c, S, P, and γ for a given θ_t are kept. From Fig. 2(a), it can be seen that the interface width of the density profile is roughly $2a$. The interface width is the narrowest at $\theta_t=\pi/2$, and it increases as the tilt angle θ_t decreases. The behavior observed here is comparable to that observed for the I-N interface of rigid rods. In general, the spatial variation of the density profile is quite smooth. The density profile for $\theta_t=\pi/2$ displays a depletion near the isotropic side of the interface. Earlier, we had found a similar dip in an analysis of the interface for rigid rods, for $\theta_t\approx0$ [12]. In both cases, the dip extends into the isotropic phase for about the size of the interfacial width. We are unable to propose a qualitative picture to explain this. Grosberg and Pachomov [11] discussed the cause of the possible nonmonotonic behavior of the interfacial profile by observing the behavior of the

orientational entropy. The profiles found here cannot be simply explained by such a discussion.

Figure 2(b) shows the order parameter profile. Unlike the density profile, the order parameter profile $S(x)$ is a monotonic function of x in general. The interfacial width of the order parameter seems broader than that of the density profiles. The center of the density profile is always slightly shifted towards the nematic phase compared to that of the order-parameter profile. The distance between the center of the density profile and that of the order-parameter profile increases as θ_t decreases. At $\theta_t=\pi/2$, it reaches the minimum. Similar behavior has been observed for the interface of rigid rods [12].

Figure 2(c) shows the profile for the biaxiality parameter $P(x)$. The biaxial effect only appears significantly in the interfacial region. It is negative on the isotropic side and positive on the nematic side. The biaxiality is strongest for $\theta_t=\pi/2$ because of the strong effect of the interface in distorting the distribution function. There is no biaxialty for the $\theta_t=0$ case because of the rotational symmetry. In general, the biaxial effect for the I-N interface is quite weak, confirming an earlier observation made by one of us [13]. In contrast, Marcus [24] investigated a Landau-expansion model and concluded that the biaxiality effect plays an important role in determining the I-N interfacial structure.

Figure 2(d) shows the director deviation angle profile. For $\theta_t=\pi/2$ and 0, we can show that $\rho_{2,1}=0$ in general. The orientation order parameter tensor in Eq. (32) is diagonalized. In these two cases, there is no change of the nematic director across the interface. For the tilt angle having other values, the deviation angle defined in Eq. (36) can be calculated. As can be seen from the figure, $\gamma(x)$ is very small. It is difficult to give a realistic error estimation for $\gamma(x)$. We are not certain about the actual existence of a deviation of the nematic director because of the smallness of the $\gamma(x)$ angle.

Figure 3 shows the dependence of the isotropic-nematic interface tension on the tilt angle θ_t between the bulk nematic director and the normal to the interface. The interface tension is a monotonic function of the tilt angle and has a minimum at $\theta_t=\pi/2$. Therefore, the excluded-volume interaction prefers to have a tilt angle of $\pi/2$ [32]. This is the same conclusion drawn earlier for rigid rods [12]. The interface tension σ at $\theta_t=\pi/2$ is given by

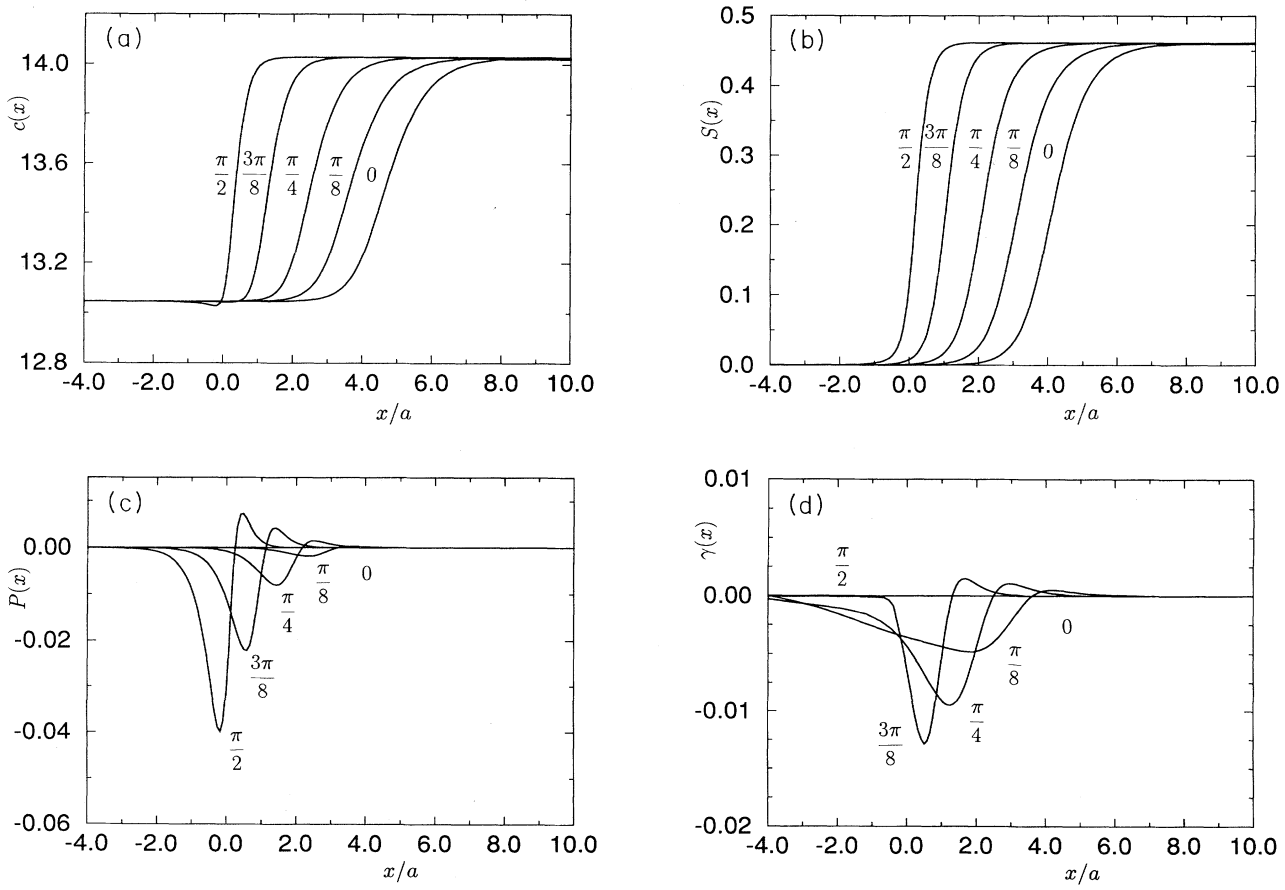

FIG. 2. (a) density profile $c(x)$, (b) order-parameter profile $S(x)$, (c) biaxiality profile $P(x)$, and (d) profile of the deviation angle $\gamma(x)$ of the nematic direction from the bulk nematic direction, at the isotropic-nematic interface. The centers of these profiles are shifted by a in order to clearly display them for different tilt angles. The tilt angles (θ_t) are indicated in the figure.

$$\sigma=(0.221\pm0.002)\frac{k_BT}{aD}\ , \tag{38}$$

which is consistent with the scaling argument given in Sec. II. The important length scale appearing in the interfacial tension and width is the Kuhn length a, or more precisely the persistent length $2a$. The total contour length L becomes important only when we need to *count* the number of effective Kuhn lengths in the system [33], such as in calculating the molecular number density. The I-N interfacial tension for semiflexible polymers can then be written as

$$\sigma=\frac{L}{D}\frac{k_BT}{\langle R^2\rangle|_{\rm KP}}\bar{\sigma}\left[\frac{L}{a}\right]\ , \tag{39}$$

where $\langle R^2\rangle|_{\rm KP}$ is the Kratky-Porod expression for the mean square end-to-end distance [34], and $\bar{\sigma}(L/a)$ is a smooth function of its argument. We know from this and previous results [12] that $\bar{\sigma}(0)=0.181$ and $\bar{\sigma}(\infty)=0.221$.

The case of $\theta_t=\pi/2$ is special, for which the surface tension exhibits a minimum. In addition to the symmetry properties discussed in Eq. (22), $q(x,\mathbf{u})$ also obeys the symmetry property $q(x,\mathbf{u})=q(x,\mathbf{u}_{\sigma_x})$ with $u_{\sigma_x}=(\pi-\theta,\phi)$. Applying this to the series expansion in (23), we can show that all the odd $l+m$ terms are absent. Therefore, we may reduce the number of the $q_{l,m}(l\le10)$ functions to 36. The reduction of this number enables us to increase the number of mesh points for x, while keeping the total variable number the same order. For $n_\xi=100$, we found $\sigma=0.220k_BT/aD$. In Fig. 4 we show the expansion coefficients $q_{l,m}$ as a function of x for $\theta_t=\pi/2$ at the interface. Since these functions are very different in magnitude, here we only plotted 24 pairs of (l,m) with absolute values greater than 1×10^{-5}.

V. SUMMARY

In this paper, we have considered an inhomogeneous free-energy model for the isotropic-nematic interface of liquid-crystalline polymers. We have developed a numerical procedure to obtain an exact numerical solution for the interfacial profile and confirmed many general expectations for the physical properties in the interfacial region caused by the repulsive excluded-volume interaction.

The basic framework to generalize the present approach to deal with semiflexible chains has already been set up in the Appendix. The actual calculation, however, demands much more work—one needs to consider the distribution function as a function of the contour coordinate because different segments have different orientational properties. We hope to report this investigation in the near future.

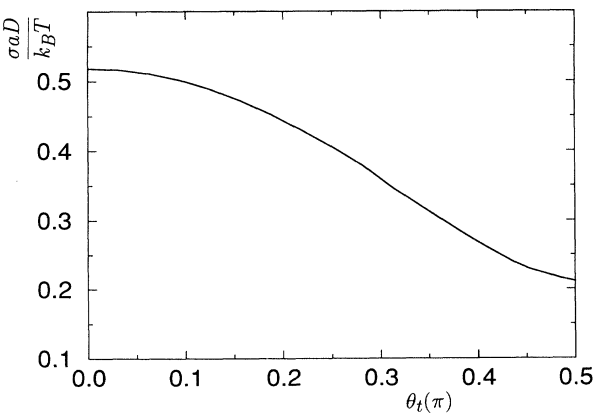

FIG. 3. The isotropic-nematic interfacial tension as a function of tilt angle θ_t.

ACKNOWLEDGMENTS

This work was supported by the National Science and Engineering Research Council of Canada.

APPENDIX: THE FUNCTIONAL INTEGRAL APPROACH

The partition function for N wormlike polymers contained in a volume V is given by

$$Z=\frac{1}{N!}\int\prod_{j=1}^{N}D(\mathbf{r}_j(t))D(\mathbf{u}_j(t))P(\mathbf{r}_j(t),\mathbf{u}_j(t))\times\exp[-W/k_BT]\ , \tag{A1}$$

where the wormlike chain is described by the statistical probability

$$P(\mathbf{r}(t),\mathbf{u}(t))\propto\exp\left[-\frac{a}{4L}\int_0^1dt\left[\frac{d\mathbf{u}(t)}{dt}\right]^2\right]\times\delta\left[\mathbf{r}(t)-\mathbf{r}(0)-\int_0^t ds\,\mathbf{u}(s)\right]\ , \tag{A2}$$

and the intermolecular potential

$$\frac{W}{k_BT}=\frac{1}{2V}\sum_{jj'}\int_0^1dt\int_0^1dt'v(\mathbf{r}_j(t),\mathbf{u}_j(t);\mathbf{r}_{j'}(t'),\mathbf{u}_{j'}(t'))\ , \tag{A3}$$

where L is the contour length and a is the Kuhn length. The interaction potential $v(\mathbf{r}_1,\mathbf{u}_1;\mathbf{r}_2,\mathbf{u}_2)$ has the Onsager form, when $L,a\gg D$:

$$v(\mathbf{r}_1,\mathbf{u}_1;\mathbf{r}_2,\mathbf{u}_2)=L^2D\delta(\mathbf{r}_1-\mathbf{r}_2)|\mathbf{u}_1\times\mathbf{u}_2|\ . \tag{A4}$$

Following the standard functional integral approach [16,35], one can now define the Green function $Q(t,\mathbf{r},\mathbf{u};\mathbf{r}_0,\mathbf{u}_0)$ for the distribution function of a polymer chain of length t to have the initial end at $(\mathbf{r}_0,\mathbf{u}_0)$ and the final end at $(\mathbf{r},\mathbf{u})$ in the phase space. The partition function $q(t,\mathbf{r},\mathbf{u})\equiv\int d\mathbf{r}_0d\mathbf{u}_0Q(t,\mathbf{r},\mathbf{u};\mathbf{r}_0,\mathbf{u}_0)$ obeys a diffusion equation in an external field $w(\mathbf{r},\mathbf{u})$ [35]

$$\frac{\partial q(t,\mathbf{r},\mathbf{u})}{\partial t}=\left[\frac{L}{a}\nabla_{\mathbf{u}}^2-L\mathbf{u}\cdot\nabla_{\mathbf{r}}-w(\mathbf{r},\mathbf{u})\right]q(t,\mathbf{r},\mathbf{u})\ . \tag{A5}$$

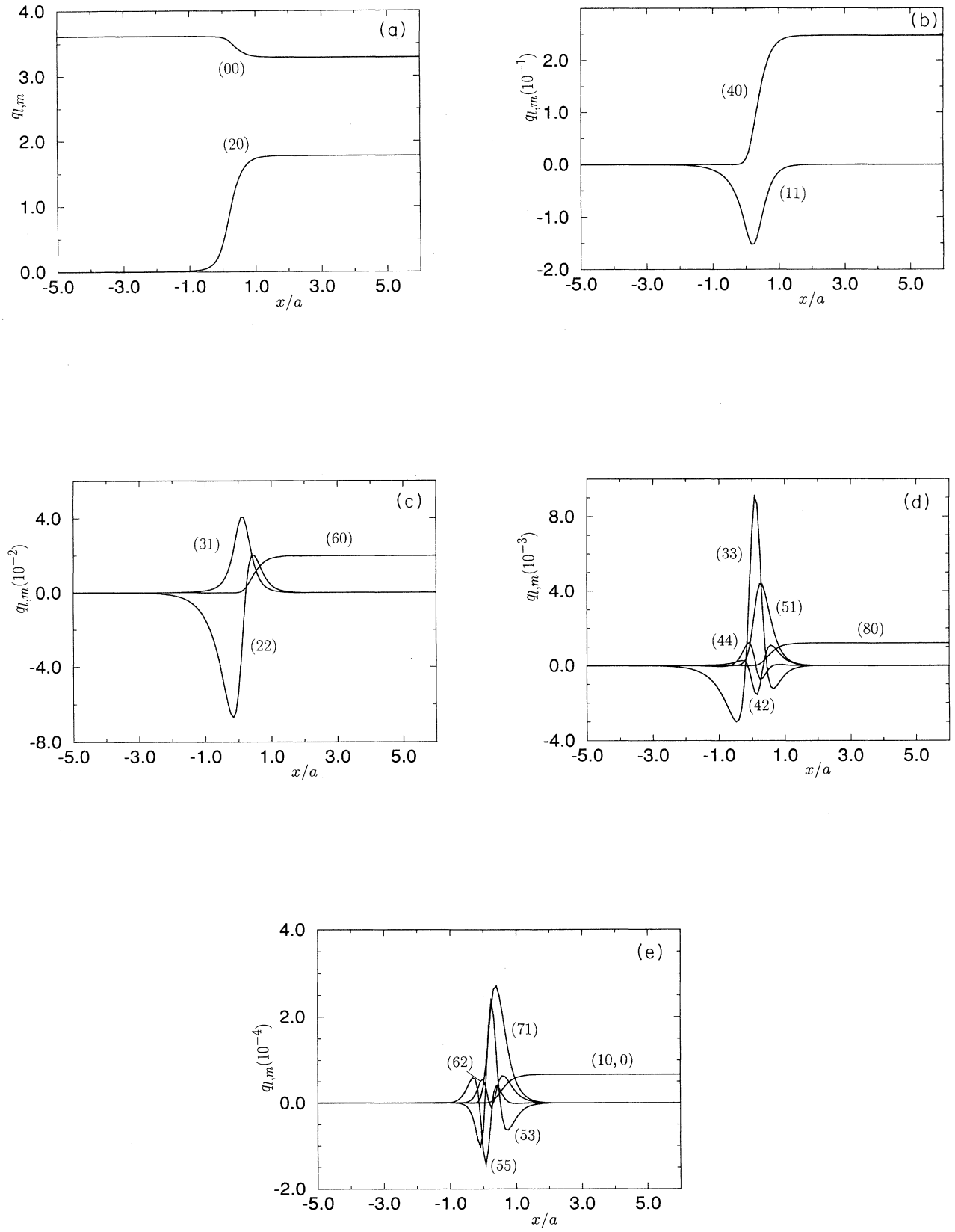

FIG. 4. The expansion coefficients as a function of x for different l and m at tilt angle $\theta_t = \pi/2$. l and m are indicated in the figure.

The total partition function of the chain is

$$Q=\int d\mathbf{r}\,d\mathbf{u}\,q(t=1,\mathbf{r},\mathbf{u})\ . \tag{A6}$$

The chain-averaged density function $\rho(\mathbf{r},\mathbf{u})$ is then determined by

$$\rho(\mathbf{r},\mathbf{u})=\frac{N}{Q}\int_0^1 dt\,q(1-t,\mathbf{r},-\mathbf{u})q(t,\mathbf{r},\mathbf{u})\ . \tag{A7}$$

Including only the Onsager-type excluded-volume interaction term, the mean-field free energy can be written as

$$\frac{F}{k_BT}=N\ln\frac{4\pi N}{Q}-\int d\mathbf{r}\,d\mathbf{u}\,w(\mathbf{r},\mathbf{u})\rho(\mathbf{r},\mathbf{u})+\frac{L^2D}{2}\int d\mathbf{r}\,d\mathbf{u}\,d\mathbf{u}'\rho(\mathbf{r},\mathbf{u})\rho(\mathbf{r},\mathbf{u}')|\mathbf{u}\times\mathbf{u}'|\ , \tag{A8}$$

where we have assumed the second virial approximation. For the rodlike limit, Eqs. (A5)–(A8) recover the extended Onsager model used to describe the inhomogeneous rigid-rod systems [9,12]. For the flexible-chain limit, $L/a\gg 1$, Eqs. (A5)–(A8) give Eqs. (1)–(3).

[1] P. G. de Gennes, Mol. Cryst. Liq. Cryst. **12**, 193 (1971).
[2] T. J. Sluckin and A. Poniewierski, in *Fluid Interfacial Phenomena,* edited by C. A. Croxton (Wiley, New York, 1986).
[3] D. Langevin and M. A. Bouchiat, Mol. Cryst. Liq. Cryst. **22**, 317 (1973).
[4] S. Faetti and V. Palleschi, Phys. Rev. A **30**, 3241 (1984).
[5] M. M. Telo de Gama, Mol. Phys. **52**, 585 (1984).
[6] M. Doi and N. Kuzuu, J. Appl. Polym. Sci., Appl. Polym. Symp. **41**, 65 (1985).
[7] H. Kimura and H. Nakano, J. Phys. Soc. Jpn. **55**, 4186 (1986).
[8] R. Holyst and A. Poniewierski, Phys. Rev. A **38**, 1527 (1988).
[9] W. E. McMullen, Phys. Rev. A **38**, 6384 (1988).
[10] B. G. Moore and W. E. McMullen, Phys. Rev. A **42**, 6042 (1990).
[11] A. Yu Grosberg and D. V. Pachomov, Liq. Cryst. **10**, 539 (1991).
[12] Z. Y. Chen and J. Noolandi, Phys. Rev. A **45**, 2389 (1992).
[13] Z. Y. Chen, Phys. Rev. E **47**, 3765 (1993).
[14] M. A. Osipov and S. Hess, J. Chem. Phys. **99**, 4181 (1993).
[15] T. Runke, B. Song, and J. Springer, Ber. Bunsenges. Phys. Chem. **98**, 508 (1994).
[16] E. Helfand, J. Chem. Phys. **62**, 999 (1975).
[17] A. J. Liu and G. H. Fredrickson, Macromolecules **26**, 2817 (1993).
[18] W. E. McMullen and K. F. Freed, J. Chem. Phys. **92**, 1413 (1990).
[19] Y. Lansac and L. Maissa, Physica **180**, 53 (1992).
[20] N. Saito, K. Takahashi, and Y. Yunoki, J. Phys. Soc. Jpn. **22**, 219 (1967).
[21] Z. Y. Chen, Macromolecules **26**, 3419 (1993).
[22] A. R. Khokhlov and A. N. Semenov, Physica A **112**, 605 (1982).
[23] L. Onsager, Ann. N. Y. Acad. Sci. **51**, 627 (1949).
[24] M. A. Marcus, Mol. Cryst. Liq. Cryst. **100**, 253 (1983).
[25] A. R. Khokhlov and A. N. Semenov, J. Stat. Phys. **38**, 161 (1985).
[26] G. J. Vroege and T. Odijk, Macromolecules **21**, 2848 (1988).
[27] J. W. Cahn and J. E. Hilliard, J. Chem. Phys. **31**, 688 (1959).
[28] L. D. Landau and E. M. Lifshitz, *Statistical Physics* (Pergamon, Oxford, 1958).
[29] T. Odijk, Macromolecules **19**, 2313 (1986).
[30] I. S. Gradshteyn and I. M. Ryzhik, *Tables of Integrals, Series, and Products* (Academic, New York, 1980).
[31] E. Isaacson and H. Bishop, *Analysis of Numerical Methods* (Wiley, New York, 1966).
[32] H. Kimura and H. Nakano, J. Phys. Soc. Jpn. **54**, 1730 (1985).
[33] In Ref. [19], the two terms Kuhn length and persistence length are taken to be synonymous.
[34] O. Kratky and G. Porod, Recl. Trav. Chim. **68**, 1106 (1949).
[35] K. F. Freed, Adv. Chem. Phys. **22**, 1 (1972).